

Reentrant spin-glass behavior in $TlFe_{2-x}Se_2$ with the $ThCr_2Si_2$ -type structure

J. J. Ying, A. F. Wang, Z. J. Xiang, X. G. Luo, R. H. Liu, X. F.

Wang, Y. J. Yan, M. Zhang, G. J. Ye, P. Cheng and X. H. Chen*

*Hefei National Laboratory for Physical Science at Microscale and Department of Physics,
University of Science and Technology of China, Hefei,
Anhui 230026, People's Republic of China*

We investigated the physical properties of $TlFe_{2-x}Se_2$ single crystals. The resistivity of $TlFe_{2-x}Se_2$ shows typical semiconductor behavior with an activation energy of 25 meV. DC susceptibility indicates an antiferromagnetic transition at about 450 K. Reentrant spin-glass (RSG) behavior was found at about 130 K through DC and AC magnetic measurements. The RSG behavior suggests the existence of a strong competition between ferromagnetic (FM) and antiferromagnetic (AFM) interactions due to Fe deficiencies. Strong electron-electron correlation may exist in this material and it is possibly a candidate of parent compound for high T_c superconductors.

PACS numbers: 75.30.Kz, 75.50.Lk, 75.60.Ej

The newly discovered iron-based superconductors have attracted much attention in past three years¹⁻⁵. All the iron-based superconductors have square planar Fe^{2+} layers. The binary chalcogenide α -FeSe with PbO-structure is found to be superconducting at 8 K⁶ and the T_c could reach 37 K under high pressure⁷. It is very meaningful to investigate other materials which contain the same Fe-Se layers. Through intercalation between the Fe-Se layers might induce high chemical pressure and strongly increases T_c . $TlFe_{2-x}Se_2$ with the $ThCr_2Si_2$ -type structure consists of Fe-Se layers which is the same with α -FeSe except for some iron deficiencies^{8,12}. The large size of Tl cation leads to larger separation between Fe-Se layers than that in α -FeSe. The structure of stoichiometric $TlFe_2Se_2$ is shown in the inset of Fig.1(a). The physical properties of this compound have not been reported except for the antiferromagnetic transition at 450 K revealed by the Mössbauer measurements¹². It is very significant to systematically investigate its physical properties and find out its relation to the high T_c superconductors. Recent research in $Fe_{1.1}Te_{1-x}Se_x$ system shows that spin-glass state would emerge when antiferromagnetic state is destabilized by the Se substitution⁹. Spin glasses (SGs) are the magnetic system in which the interactions between the magnetic moments are in conflict with each other, thus no conventional long-range order can be established¹⁰.

In this paper, we investigated the physical properties of the $TlFe_{2-x}Se_2$ single crystals. The resistivity shows typical semiconductor-like behavior with the activated energy of 25 meV and no superconductivity was found. Antiferromagnetic transition was also detected by the DC susceptibility measurement at about 450 K. Reentrant spin-glass (RSG) behavior was found at about 130 K through DC and AC magnetic measurements. RSG transition is a well-known phenomenon of spin glasses.

The RSG system known thus far has either long-range FM or AFM ordering above the spin glass transition temperature¹¹. This behavior may be related to the competition between ferromagnetic and antiferromagnetic interactions in the iron layers.

$TlFe_{2-x}Se_2$ single crystals were grown by directly melting the mixture of Tl_2Se , Fe and Se powders in the sealed quartz tube at the temperature of 800°C. After keeping the mixture at 800°C for 2 days, the furnace was slowly cooled down to 500°C at the rate of 5°C/h, then the power of furnace was shut off. Plate like single crystals of $TlFe_{2-x}Se_2$ can be easily cleaved from the final product. Energy-dispersive X-ray spectroscopy (EDX) shows the iron deficiency x is about 0.35.

Single crystal of $TlFe_{2-x}Se_2$ was characterized by x-ray diffractions (XRD) using Cu K_α radiations. As shown in the Fig.1(a). Only (00 l) diffraction peaks were observed, suggesting that the crystallographic c axis is perpendicular to the plane of the single crystal. The lattice constant of c -axis is determined to be 13.98 Å which is slightly smaller than the reported value 14.00 Å. Fig.1(b) shows the temperature dependence of the resistivity with the electric current flowing in the ab plane of the $TlFe_{2-x}Se_2$ single crystal. The resistivity increases rapidly with decreasing the temperature and the room-temperature resistivity is about 5 mΩ*cm. The red line in the inset of Fig.1(b) is the linear fit of $\log(\rho)$ versus $1/T$. The resistivity behavior basically obeys the thermally activated behavior: $\rho = \rho_0 \exp(E_a/k_B T)$, where ρ_0 refers to a prefactor and k_B is Boltzmann constant. The activation energy E_a was estimated to be about 25 meV from the fitting result. However, density functional calculation shows that $TlFe_2Se_2$ has density state at the Fermi surface, and should be metallic. This is very different from our results¹³. This contradiction could be due to the Fe deficiency in our samples or the strong electron correlation in $TlFe_{2-x}Se_2$.

Fig.2(a) shows the temperature dependence of the DC magnetic susceptibility above 300 K with the magnetic field of 5 T applied along the ab plane. The sudden drop

*Corresponding author; Electronic address: chenxh@ustc.edu.cn

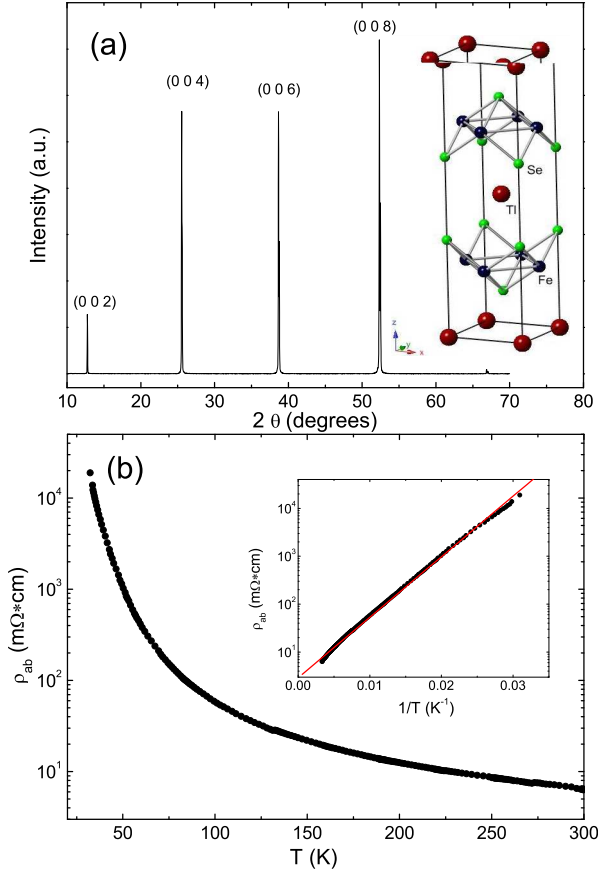


FIG. 1: (color online). (a): The single crystal x-ray diffraction pattern of $TlFe_{2-x}Se_2$. Only (00l) diffraction peaks show up indicating that the c axis is perpendicular to the plane of the plate. The inset shows the crystal structure of stoichiometric $TlFe_2Se_2$, the red, blue and green balls represent Tl, Fe and Se ions. (b): Temperature dependence of the in-plane resistivity. The inset shows that $\text{Log}(\rho)$ can be linearly fitted with $1/T$. The red line is the linear fitting result.

of the magnetic susceptibility at about 450 K indicates the antiferromagnetic ordering below 450 K. This result is consistent with the previous report by Mössbauer measurements¹². Fig.2(b) shows the anisotropic magnetization measurements with the applied field of 100 Oe parallel and perpendicular to the ab plane below 300 K. A pronounced irreversibility between the zero-field-cooling (ZFC) and field-cooling (FC) curves can be observed below 130 K. It definitely indicates a second magnetic transition. This second magnetic transition behaves actually like a spin-glass transition. The ZFC curve shows a cusp-like behavior with the peak at about 130 K and the FC curve becomes almost a constant below the reentrant spin-glass transition temperature T_{RSG} (We defined the T_{RSG} as the peak of the ac susceptibility at about 130 K shown in Fig.3) due to the spin freezing. The mag-

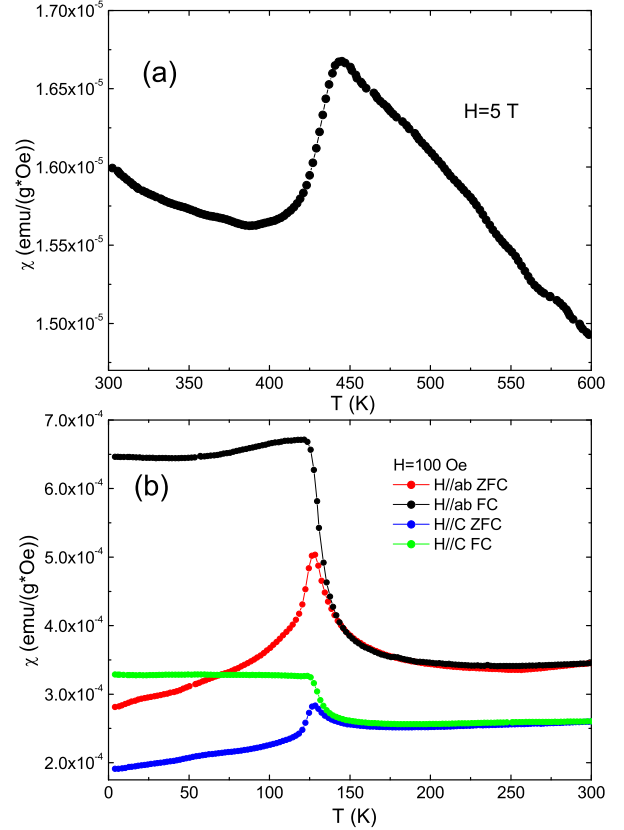


FIG. 2: (color online). (a): The DC magnetic susceptibility with the applied field of 5 T along the ab plane above 300 K. (b) ZFC and FC magnetic susceptibility with the magnetic field applied parallel and perpendicular to the plane below 300 K, respectively.

netic susceptibility for the field applied in the ab plane is about twice in magnitude larger than that with the field applied perpendicular to the ab plane. It suggests that magnetic moments in the iron plane prefer to align along the ab plane, being consistent to the Mössbauer measurements and the theoretical calculation^{12,13}. The susceptibility almost does not change with decreasing the temperature above 200 K due to the nature of the long-ordering AFM state. With the temperature approaching T_{RSG} , the susceptibility increases very rapidly with the magnetic field applied both along and perpendicular to the ab plane. It might be due to an increase of the ferromagnetic interactions in the iron layers around T_{RSG} . Actually, the ferromagnetic interactions start to emerge at the temperature much higher than T_{RSG} as the susceptibility starts to increase at the temperatures much higher than T_{RSG} .

Fig.3(a) and (b) show the real part of ac magnetic susceptibility with the frequency of 1 Hz with the ac magnetic field ($H_{ac} = 3.8$ Oe) parallel and perpendicular to the ab plane, respectively. The real part of ac magnetic

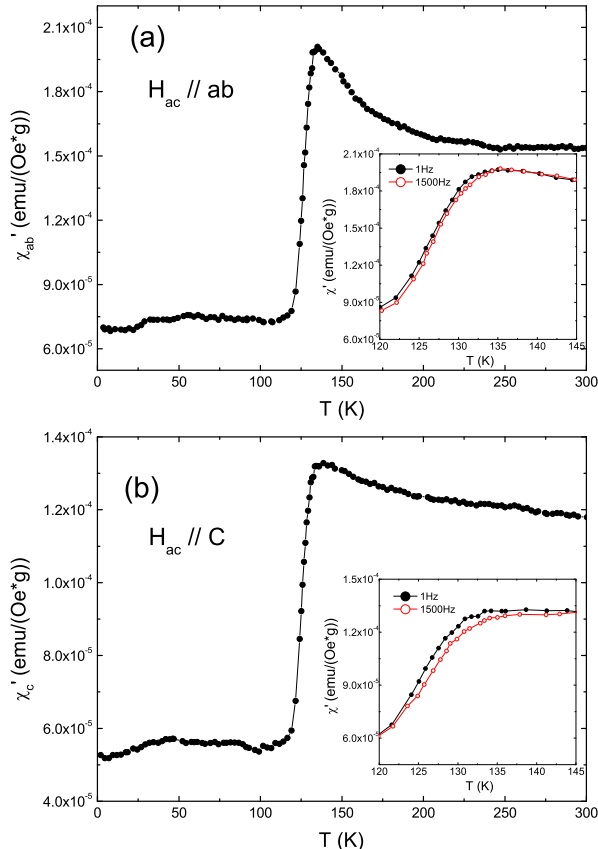


FIG. 3: (color online). The real part of ac susceptibility with the frequency of 1 Hz with the ac field applied along and perpendicular to the plane (a) and (b), respectively. The insets show the frequency shift around the RSG transition temperature. The red line is the ac susceptibility with the frequency of 1500 Hz.

susceptibility slightly increases with decreasing the temperature at high temperature and shows a peak at about 130 K. The sharp drop in ac susceptibility below T_{RSG} indicates the spin freezing below T_{RSG} . T_{RSG} shifts to higher temperature with increasing the frequency to 1500 Hz as shown in the inset of Fig.3(a) and (b). This behavior strongly supports the glassy nature of the magnetic state in this system. Larger value of χ'_{ab} than χ'_c also indicates that the magnetic moments prefer to align along the ab plane.

To further investigate the RSG behavior, we measured the long-time relaxation of the DC magnetization. Fig.4 (a) and (b) show the long-time relaxation behavior of $M_{ZFC}(t)$ for the magnetic field applied parallel and perpendicular to the ab plane, respectively. The experiment process is as follows. The crystal was cooled without magnetic fields (the ZFC process) from the room temperature to 4 K ($<T_{RSG}$), then the magnetic field of 100 Oe was applied parallel or perpendicular to the plane. As

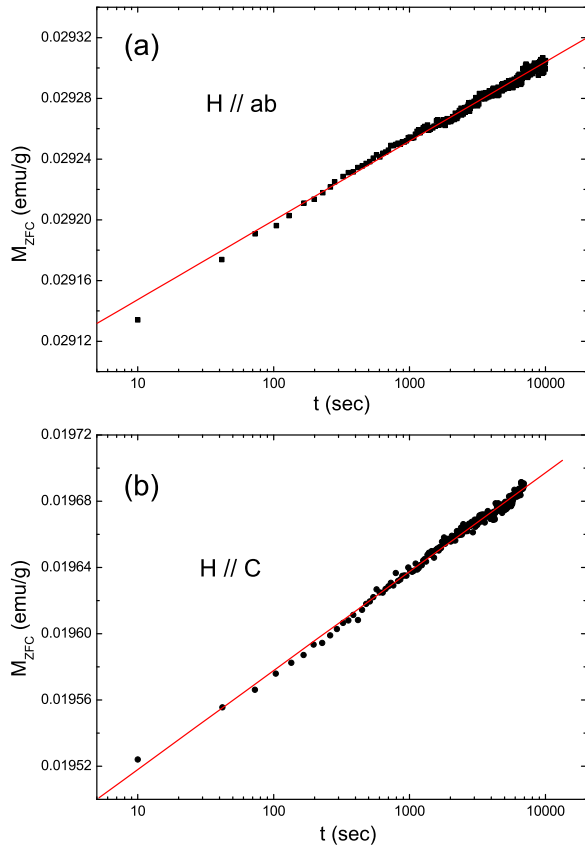


FIG. 4: (color online). The long-time relaxation behavior of $M_{ZFC}(t)$ for the magnetic field applied parallel (a) and perpendicular (b) to the ab plane. The red line is the linear fitting of the M_{ZFC} with $\log(t)$.

soon as the field was applied, the M_{ZFC} was measured as a function of time t . As shown in Fig.4(a) and (b), it is found that the M_{ZFC} slowly increases almost linearly with the $\log(t)$. The long-time relaxation evidences an important role of the frustration as observed in the SG region of $La_{1-x}Sr_xCoO_3$ perovskite compounds^{14,15}. This long-time relaxation behavior in the low temperature region is consistent with the RSG state¹⁶⁻¹⁸.

Fig.5(a) and (b) show the magnetization hysteresis curves for the magnetic field applied parallel and perpendicular to the ab plane, respectively. An S-shape M-H Loop is observed at 120 K which is a little lower than T_{RSG} . This behavior is typical in SG system. The magnitude of coercive fields are 100 Oe and 150 Oe for the magnetic field applied parallel and perpendicular to the plane, respectively. While above T_{RSG} , only unobvious loop can be found. This behavior may be attributed to the competition between ferromagnetic and antiferromagnetic interactions. Above T_{RSG} antiferromagnetic is much stronger than ferromagnetic interactions. While below T_{RSG} , ferromagnetic interaction is comparable to

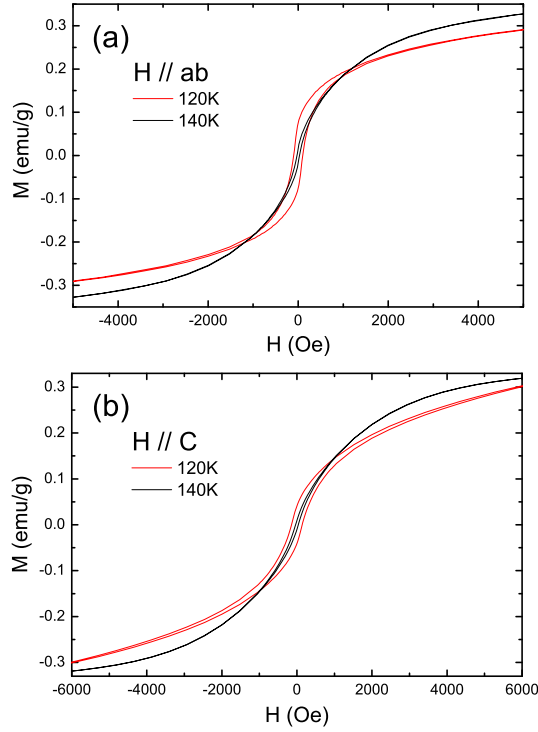


FIG. 5: (color online). Isothermal magnetization hysteresis loop with the magnetic field applied parallel (a) and perpendicular (b) to the ab plane. The red hysteresis curve is at 120 K below T_{RSG} and the black one is at 140 K above T_{RSG} .

b

the antiferromagnetic interaction, some part of the system may form domains. Thus due to the blocking of the domain wall motion similar to ferromagnetic materials M-H loop occurs. The competition of ferromagnetic interaction and the antiferromagnetic interaction may be the main cause of the RSG transition. The s-shape M-H loop above T_{RSG} also indicate that the short-range ferromagnetic interaction already exist above T_{RSG} and the strong fluctuation in this system.

In order to further investigate the spin-glass transition at around 130 K, we performed heat capacity measurement at the temperature range from 4 K to 200 K. Fig.6 shows the result of the heat capacity for $TlFe_{2-x}Se_2$. A very weak broad hump of C_p/T extending over a wide temperature range can be found around T_{RSG} as shown in the inset of Fig.6. It confirms that the transition around 130 K is the bulk property for the $TlFe_{2-x}Se_2$. Such a broad hump of the heat capacity is often observed in spin-glass system^{19,20}.

The spin-glass behavior has been reported in $FeSe_{1-x}Te_x$ system⁹. A Similar SG state is found in the $TlFe_{2-x}Se_2$ with $ThCr_2Si_2$ structure. The RSG state in the $TlFe_{2-x}Se_2$ is mainly attributed to arise from the competing interactions between the FM and

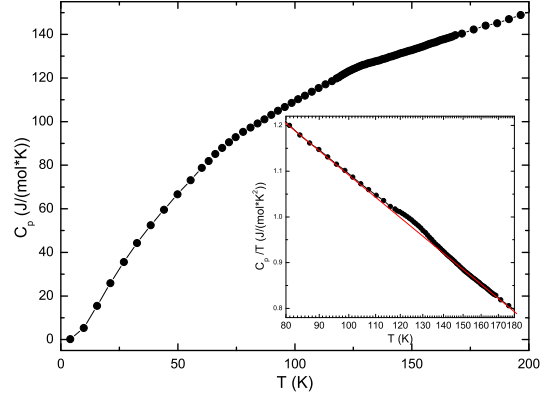


FIG. 6: (color online). Temperature dependence of the heat capacity. The inset is the enlarged area around T_{RSG} of C_p/T . The red line is the contrast line for us to easily detect the broad hump around T_{RSG} .

AFM phases. Mössbauer measurement shows that the antiferromagnetic transition temperature is greatly suppressed and the transition width broaden with increasing the iron vacancy²¹. It suggests that the iron vacancies would strongly destroy the antiferromagnetic ground state of the the Fe ion layers, and the fluctuation is induced between the neighbor Fe ions around the Fe vacancies. The spin-glass like behavior was also found in the isostructure compounds $ACuFeS_2$ ($A=K, Rb, Cs$), they can be represented as micromagnets at low temperature and the superexchange interactions between spins within a cluster depend on the distribution of iron ions²². In our system, the Fe vacancies may separate the Fe spins and Fe cluster can be formed, consequently lead to the spin glass state. All these results indicate that the Fe ion deficiencies may be the origin of the RSG behavior in $TlFe_{2-x}Se_2$. The semiconductor-like resistivity is quite different to the metal state for the material without iron deficiencies calculated by density functional calculation. The typical semiconductor resistivity behavior is also found in $ACuFeS_2$. The non-linear M-H curve indicates the strong fluctuation in the iron layers. The high antiferromagnetic transition temperature and insulator ground state is very similar to the parent compounds of cuprates. Strong electron correlation may exist in this kind of material and it is possibly a candidate of parent compounds for high T_c superconductors. In order to explore superconductivity in this material, the problem is how to overcome the Fe deficiency in the iron-layers.

In conclusion, we systematically investigated the physical properties of the $TlFe_{2-x}Se_2$ single crystals. The resistivity shows typical semiconductor behavior, and no superconductivity was found at the temperature cooling down to 2 K. At 450 K, antiferromagnetic transition was observed by DC magnetic measurement, being consistent with the early Mössbauer result. Both DC and AC mag-

netic measurements show the RSG transition at the temperature around 130 K. The RSG state could arise from the competition between the FM and AFM interactions. Such competing interactions may be due to the iron deficiencies, and such deficiencies induce the fluctuation between the neighbor Fe ions around the Fe vacancies. The heat capacity shows a very small and broad hump with

no resemblance to a λ -type peak around the T_{RSG} . This material might be a candidate of parent compounds for high T_c superconductors with the same structure to the 122 phase in iron based superconductors.

This work is supported by the Nature Science Foundation of China, and by Ministry of Science and Technology and by Chinese Academy of Sciences.

-
- ¹ Y. Kamihara, T. Watanabe, M. Hirano, and H. Hosono, *J. Am. Chem. Soc.* **130**, 3296(2008).
- ² X. H. Chen, T. Wu, G. Wu, R. H. Liu, H. Chen and D. F. Fang, *Nature* **453**, 761(2008).
- ³ Z. A. Ren, G. C. Che, X. L. Dong, J. Yang, W. Lu, W. Yi, X. L. Shen, Z. C. Li, L. L. Sun, F. Zhou and Z. X. Zhao, *Europhys. Lett.* **83**, 17002(2008).
- ⁴ R. H. Liu, G. Wu, T. Wu, D. F. Fang, H. Chen, S. Y. Li, K. Liu, Y. L. Xie, X. F. Wang, R. L. Yang, L. Ding, C. He, D. L. Feng and X. H. Chen, *Phys. Rev. Lett.* **101**, 087001 (2008).
- ⁵ M. Rotter, M. Tegel, D. Johrendt, *Phys. Rev. Lett.* **101**, 107006(2008).
- ⁶ F.-C. Hsu, J.-Y. Luo, K.-W. Yeh, T.-K. Chen, T.-W. Huang, P. M. Wu, Y.-C. Lee, Y.-L. Huang, Y.-Y. Chu, D.-C. Yan, and M. K. Wu, *Proc. Natl. Acad. Sci. U.S.A.* **105**, 14262 (2008).
- ⁷ S. Medvedev, T. M. McQueen, I. A. Troyan, T. Palasyuk, M. I. Erements, R. J. Cava, S. Naghavi, F. Casper, V. Ksenofontov, G. Wortmann, and C. Felser, *Nature Mater.* **8**, 630 (2009).
- ⁸ K. Klepp, H. Boller, *Mh Chemie* **109**, 1049-1057 (1978).
- ⁹ P. L. Paulose, C. S. Yadav, K. M. Subhedar, *Europhysics Letters*, **90**, 27011 (2010).
- ¹⁰ K. Binder and A. P. Young, *Rev. Mod. Phys.* **58**, 801 (1986)
- ¹¹ I. A. Campbell, S. Senoussi, F. Varret, J. Teillet and A. Hamzic, *Phys. Rev. Lett.* **50**, 1615 (1983).
- ¹² L. Häggström, H. R. Verma, S. Bjarman, R. Wäppling, and R. Berger, *J. Solid State Chem.* **63**, 401 (1986).
- ¹³ Lijun Zhang and D. J. Singh, *Phys. Rev. B* **79**, 094528 (2009)
- ¹⁴ M. Itoh, I. Natori, S. Kubota, and K. Motoya, *J. Phys. Soc. Jpn.* **63**, 1486 (1994).
- ¹⁵ D. N. H. Nam, K. Jonason, P. Nordblad, N. V. Khiem, N. X. Phuc, *Phys. Rev. B* **59**, 4189 (1999).
- ¹⁶ Joonghoe Dho, W. S. Kim, and N.H. Hur, *Phys. Rev. Lett.* **89**, 027202 (2002).
- ¹⁷ K. Jonason, J. Mattsson, and P. Nordblad, *Phys. Rev. Lett.* **77**, 2562 (1996).
- ¹⁸ R. Mathieu, P. Jonsson, D. N. H. Nam, and P. Nordblad, *Phys. Rev. B* **63**, 092401 (2001).
- ¹⁹ G. E. Brodale, R. A. Fisher, W. E. Fogle, N. E. Phillips, and J. van Curen, *J. Magn. Mater.* **31-34**, 1331 (1983)
- ²⁰ Luis Ortega-San Martin, Jon P. Chapman, Luis Lezama, José J. Saiz Garitaonandia, Jorge Sánchez Marcos, Jesús Rodríguez-Fernández, María I. Arriortua and Teófilo Rojo, *J. Mater. Chem.* **16**, 66 (2006)
- ²¹ L. Häggström, A. Seidel, and R. Berger, *Hyperfine Interactions* **54**, 563 (1990).
- ²² M. Oledzka, K.V. Ramanujachary and M. Greenblatt, *Materials Research Bulletin*, **31**, 1491 (1996).